Thermo-Mechanical Analysis of a Copper Mould for Continuous Casting of Steel

M. Ansoldi[1], G. Bazzaro[1], D. Benasciutti[2], F. De Bona[2], G. Luvarà[1], L. Moro[2], M. Gh. Munteanu[2], F. Vecchiet[1]

[1] Centro Ricerche Danieli, Buttrio (UD), Italy

[2] Department of Electrical, Management and Mechanical Engineering, University of Udine, Italy

Email address: denis.benasciutti@uniud.it

Abstract: This work deals with the thermo-mechanical analysis of a copper mould. In the continuous casting process molten steel flows through a water-cooled mould which induces the solidification of the outer shell. The inner part of the mould undergoes a huge thermal flux and large temperature gradients develop across the copper inducing high stress and plastic deformation, especially in the region close to the meniscus. After the operating period, a cooling to room temperature induces residual stresses which may increase with repeated thermal cycling over a campaign. Another source of cyclic thermal loading during operative condition is represented by the fluctuation of melt metal level into copper mould, with a resulting variation of the temperature peak on the surface of the mould. In this work the structural behaviour of the mould under thermal loading condition is analyzed adopting a three-dimensional finite-element model, with the aim of performing an accurate evaluation of stress and strain levels. An analytical structural model is then developed with the aim of performing a sensibility analysis in the design phase. A simplified thermal fatigue approach has also been followed, in order to gain insights into cyclic behaviour and improve mould life.

Key words: continuous casting mould, thermal stress, total strain range, fatigue life.

1. INTRODUCTION

In the last few years, the demand of a strong improvement in term of productivity and reliability, accompanied by cost reduction have been fundamental requirements in the design of steelmaking equipment. The well established practice of over sizing the most critical mechanical elements can not be followed anymore, and the necessity to consider such complex phenomena as plasticity, creep, low-cycle thermal fatigue, phase transition is crucial in order to improve the life of the mechanical parts, to gain safety, and to assure high steel quality [1, 2].

This work focuses on the mould design, a crucial component for the process of continuous casting of steel. The mould (or crystallizer) controls the shape and the initial solidification of steel, governing heat transfer and the surface quality of the product. A reliable, crack-free mould within close dimensional tolerances is a key factor to guarantee a suitable level of safety, reliable quality and top productivity. The molten steel induces high thermal fluxes and temperature gradients into the copper, which in turn generate high stress levels. Subsequent sequences with start-ups and shut-downs, as well as free-surface (meniscus) oscillations during normal service, lead to cyclic thermal loading which may damage the mould [3, 4].

The aim of this work is to understand the mechanical behaviour of the mould under thermal loads, in order to relate stress-strain cycles to the life of the component and to identify the actions that can improve its durability.

2. COMPONENT DESCRIPTION

The mould is a mechanical component through which the molten steel flows. It is designed to solidify a thin shell of metal that is continuously withdrawn away up to a complete through thickness solidification. Different cross sections may be adopted (square, rectangular or rounded shapes) according the final geometry of the product (billets, blooms or slabs).

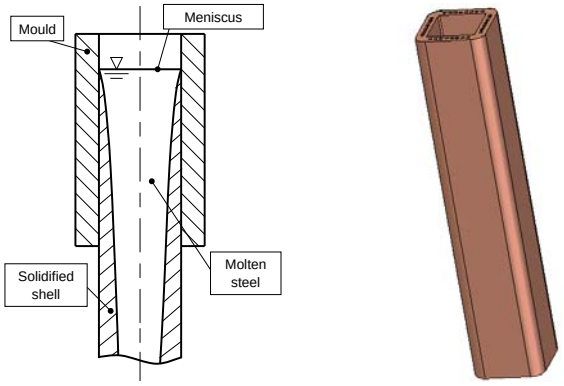

Figure 1. Geometry of the component

The main function of the mould is to provide an intensive cooling of the steel to achieve a robust shell of metal. It is required a precise control of the shape to match the shell contraction and to guarantee the product geometry. High dimensional stability at any operational regime is therefore a requirement of primary relevance.

Conventional moulds consist of a copper tube surrounded by a steel jacket: in the gap between the two elements cooling water flows [5]. In order to improve the thermo-mechanical performances, a different design configuration of the mould has been developed. It consists of a thicker copper tube provided with drilled holes for cooling. In this way a high stiffness with excellent heat transfer capacity are achieved at the same time. This work focuses on this enhanced type of mould, schematically represented in Figure 1.

3. EXPERIMENTAL INVESTIGATION OF A MOULD AFTER SERVICE

Due to the presence of molten steel, the inner part of the mould is subjected to a high thermal flux, with a characteristic profile decreasing from top to bottom. The peak values of heat flux are found to be in the proximity of the meniscus region, while lower values are experienced when the steel shell becomes thicker. The meniscus zone is found to be the most critical for the component: several works in literature account for the presence of cracks in this location. Sometimes cracks were observed after only 2 or 3 casting sequences [4].

Figure 2. Inner mould surface with closed view of the meniscus region with cracks

In thin-slab continuous casters the mould surface is periodically machined to remove cracks [6], but for billet casting this practice cannot be adopted due to restrictions in the cross section. Figure 2 shows the inner surface of a mould after several sequences of production at 30% productivity higher than conventional. The portion of the mould subjected to higher heat loads clearly appears as a darker surface. As enhanced by the extended view, in this region several micro-cracks appear after operation.

Figure 3. Manufacturing operation to obtain the tensile-test specimens.

In order to characterize the mechanical properties of the copper alloy after use, more than 20 test specimens have been obtained (see Figure 3) in different locations. The results of the tensile tests are reported in Table 1.

Table 1: Mechanical characteristics of CuCrZr alloy

	Mean value	**Standard deviation**
Modulus of elasticity	130 [GPa]	-

Yield strength	260 [MPa]	21
Ultimate tensile strength	320 [MPa]	17
Ductility (Eq. 8)	0.84	0.05

The values obtained show a limited scatter confirming that the material properties are not significantly affected by service condition.

4. THERMAL LOADING OF THE MOULD

The component undergoes two different classes of loading cycles (see Figure 4 and Figure 5). The first one, which may be referenced as macro-cycle, is characterized by a load cycle between the condition of uniform room temperature and that one corresponding to the maximum heat flux during the steady production. It represents the interval time production between a sequence start-up and shut-down.

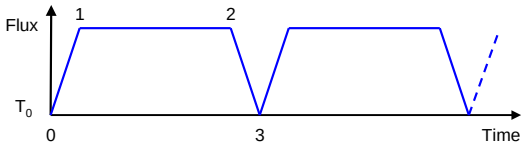

Figure 4. Scheme of the load macro-cycle

The second loading condition, which may be named micro-cycle, is representative of metal-level fluctuations normally occurring during casting conditions.

Whereas the first case occurs in a quite long period of time compared to that required to achieve the steady state condition, in the second case the frequency is high enough to establish a continuous shift in the temperature map across the nominal meniscus position. For this reason, whether in the former case a static thermal analysis could be a satisfactory approximation, for this latter condition a transient thermal analysis is compulsory, as long as a full steady state condition is never established.

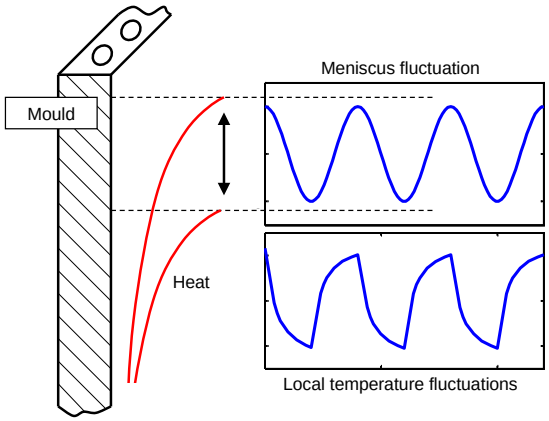

Figure 5. Scheme of micro-cycle

5. THERMO-MECHANICAL ANALYSIS: NUMERICAL RESULTS AND SIMPLIFIED ANALYTICAL MODELS

The component is characterized by 4 planes of symmetry, therefore it is possible to adopt a reduced model as represented in Figure 6. Even if a plane approach could be useful as a preliminary thermo-mechanical analysis, due to the non-uniform distribution of the thermal flux in the direction of the mould longitudinal axis, a three-dimensional (3D) model is necessary.

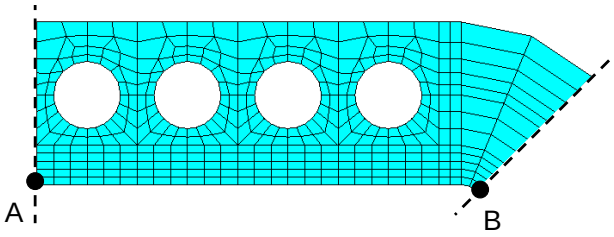

Figure 6. Top view of 3-D FE mechanical model

The thermal analysis is performed considering an imposed thermal flux acting on the inner part of the mould. The outer surface is characterized by adiabatic condition. A convective boundary condition is imposed in the inner surface of the water cooling channels. A non-linear thermal analysis is required in order to take into account the variation of thermal conductivity and specific heat with temperature.

As the problem is uncoupled, a subsequent mechanical analysis is performed imposing the nodal temperature distribution obtained from the previous analysis. The in-plane and axial thermal expansion of the component are allowed. It follows that stress-strain behaviour depends only on the internal temperature distribution. Also in this case a non-linear analysis is required. In fact the dependence of Young's modulus and yield stress with temperature needs to be considered. According to [7] starting from the measured values presented in Table 1a correlation with temperature is imposed.

In this section a linear elastic behaviour is previously considered, in order to gain insights in the physic of the problem. As it will be shown in the following, in the most critical portion of the mould, stresses exceed the elastic limit and therefore an elastic-plastic model is needed. For this purpose a bilinear model with Von Mises plasticity and kinematic hardening rule will be adopted. The results of the elastoplastic analysis, which differ from the linear case only in limited localized areas, will be presented in the following section.

Figure 7 shows the temperature distribution obtained at the maximum flux in the steady state condition. It can be noticed that the maximum temperature occurs in the region close to the meniscus. If a section orthogonal to the mould axis in proximity of the meniscus is considered, it can be shown that a relevant "radial" temperature gradient occurs up to the inner portion of the cooling pipes. In the outer part of the mould a quite constant room temperature is observed.

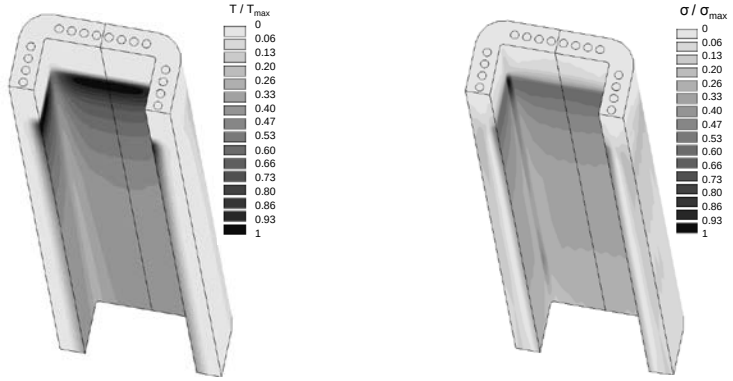

(a) (b)

Figure 7. Temperature (a) and stress (b) distribution during operative condition

Figure 7(b) shows the Von Mises stress distribution corresponding to the previous thermal analysis. It can be noticed that the maximum stress occurs close to the corner (point B in Figure 6), although higher temperatures occur at point A. The outer part of the mould shows a uniform negligible stress state. The stress distribution around point B can be interpreted using a simple

structural model which refers to a square frame filleted at the corners undergoing a thermal gradient across its thickness. If the temperature variation is linear it causes a uniform bending moment and therefore maximum stresses occur at the corners which behave as curved beams. Figure 8 shows the "hoop" stress variation along the thickness evaluated with the finite element (FE) model (r_e represents the outer curved beam radius), compared with that obtained according to Winkler theory [8]: a quite good agreement can be noticed.

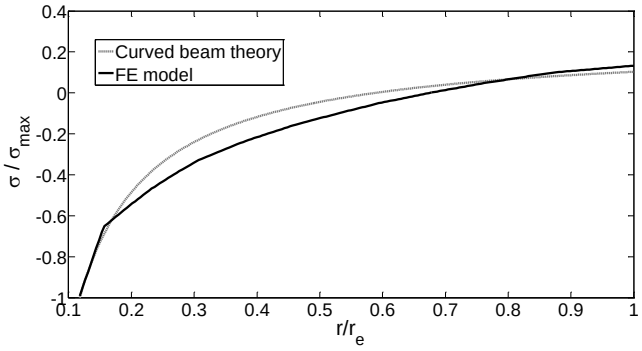

Figure 8. Stress variation along the thickness at the corner

Even if stress in point B reaches the maximum value, it occurs in the colder portion of the inner part of the component (see Figure 7), at a safe distance from water. It follows that the most critical portion of the mould is located at the meniscus mid-face (point A).

In order to develop an interpretative model of stress distribution in this area it is useful to investigate the principal stress pattern along the thickness.

In Figure 9 are represented respectively axial, "hoop" and "radial" stresses (i.e. the principal stresses in the axial direction and those contained in a plane orthogonal to the longitudinal axis and respectively parallel and perpendicular to the inner mould surface). It can be noticed that the latter stress assumes negligible values in the whole range. In the inner mould surface axial and "hoop" stresses show similar compressive values which decrease almost linearly maintaining quite comparable values.

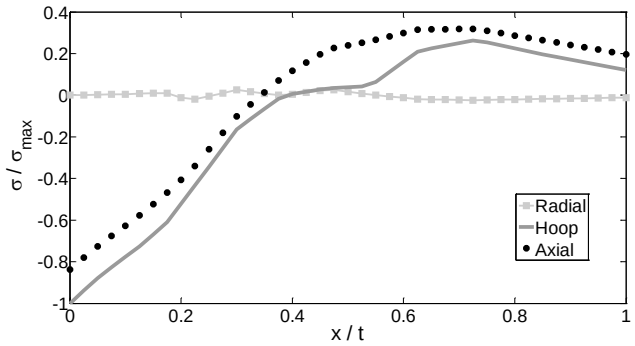

Figure 9. Stress variation through the thickness in the hottest part

It can therefore be concluded that the hottest portion of the mould undergoes a plane hydrostatic state of stress. A possible interpretative model can be developed considering the inner surface of the mould as a semi-infinite plane where a single point located on the surface is heated at temperature *T*. As it is well know the solution in term of stresses is:

$$\sigma_a = \sigma_h = -\frac{\alpha E \Delta T}{1-\nu},\ \sigma_r = 0 \qquad (1)$$

In other words a small heated part would freely expand but it is "laterally" constrained by the surrounding large cold portion.

Figure 10 shows the principal stress evaluated on the mould surface along the axial direction (*y*=0 corresponds to the upper edge of the mould whose height is *l*). It can be clearly noticed that a plane hydrostatic stress state still occurs and it is directly proportional to temperature, according to Eq. (1). From a physical point of view the component can therefore be considered as constituted by two layers: an inner hot layer (that would expand) constrained by a colder layer that is maintained at low temperature by water cooling.

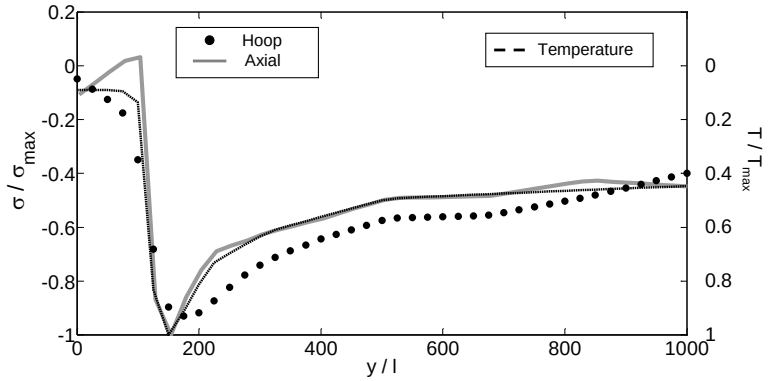

Figure 10. Principal stress on the mould surface along the axial direction.

It is thus possible to conclude that a suitable interpretative structural model of the stress and strain status in the area surrounding point A could be that of a hollow cylinder whose external part (from a radius r_f corresponding to the position of inner surface of the water channel) is maintained at constant temperature.

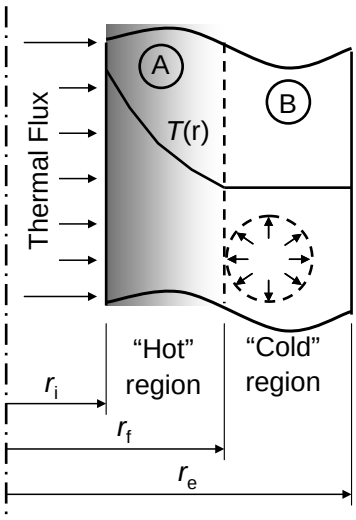

Figure 11. Hollow cylinder constituted by a "hot" and a "cold" part.

The inner surface undergoes a thermal flux which produces a variation of temperature according to the following relation:

$$\begin{cases} T^A(r) = \dfrac{T_i - T_f}{\log\left(\dfrac{r_i}{r_f}\right)} \log\left(\dfrac{r}{r_f}\right) + T_f & r < r_f \\ T^B(r) = T_f & r > r_f \end{cases} \tag{2}$$

The stress distribution and the radial displacement can thus be obtained considering the structure as composed by two parts. By following the procedure proposed in [9] for the case of a hollow cylinder clamped at its ends and undergoing a given temperature distribution, the solution has the following expression:

$$\begin{aligned}
\sigma_{\vartheta} &= +\frac{\alpha E}{1-\nu}\frac{1}{r^2}\int_{r_\mathrm{i}}^{r} T(r) r\,dr - \frac{\alpha E T(r)}{1-\nu} + \frac{E}{1+\nu}\left(\frac{C_1}{1-2\nu} - \frac{C_2}{r^2}\right) \\
\sigma_{\mathrm{r}} &= -\frac{\alpha E}{1-\nu}\frac{1}{r^2}\int_{r_\mathrm{i}}^{r} T(r) r\,dr + \frac{E}{1+\nu}\left(\frac{C_1}{1-2\nu} - \frac{C_2}{r^2}\right) \\
\sigma_{\mathrm{z}} &= -\frac{\alpha E T(r)}{1-\nu} + \frac{2EC_1}{(1+\nu)(1-2\nu)} \\
u &= \frac{1+\nu}{1-\nu}\alpha\frac{1}{r}\int_{r_\mathrm{i}}^{r} T(r) r\,dr + C_1 r + \frac{C_2}{r}
\end{aligned} \tag{3}$$

In this case, due to the fact that the temperature is described by two functions four constants C_i have to be determined. The values of C_i can be analytically obtained by imposing at the interface (r=r_i) the compatibility condition in terms of radial displacements and the continuity of stresses:

$$\begin{cases}
\sigma_{\mathrm{r}}^{\mathrm{A}}(r_\mathrm{i}) = 0 \\
\sigma_{\mathrm{r}}^{\mathrm{B}}(r_\mathrm{e}) = 0 \\
\sigma_{\mathrm{r}}^{\mathrm{A}}(r_\mathrm{f}) = \sigma_{\mathrm{r}}^{\mathrm{B}}(r_\mathrm{f}) \\
u^{\mathrm{A}}(r_\mathrm{f}) = u^{\mathrm{B}}(r_\mathrm{f})
\end{cases} \tag{4}$$

In this way the expression of C_1, C_2 and $C_1^{'}$ $C_2^{'}$ can be obtained respectively for the inner and the outer part:

$$\begin{aligned}
C_2 &= \frac{\dfrac{\alpha}{1-\nu}\dfrac{1}{r_\mathrm{f}^2}M_2 + \dfrac{1}{1+\nu}\dfrac{1}{M_3}\left(\dfrac{1+\nu}{1-\nu}\alpha\dfrac{1}{r_\mathrm{f}}M_2 - M_1 r_\mathrm{f}\right)\left(\dfrac{1}{r_\mathrm{e}^2} - \dfrac{1}{r_\mathrm{f}^2}\right) + \dfrac{1}{(1+\nu)(1-2\nu)}M_1}{\dfrac{1}{1+\nu}\left(\dfrac{1}{r_\mathrm{i}^2} - \dfrac{1}{r_\mathrm{f}^2}\right) - \dfrac{1}{1+\nu}\dfrac{1}{M_3}\left((1-2\nu)\dfrac{r_\mathrm{f}}{r_\mathrm{i}^2} + \dfrac{1}{r_\mathrm{f}}\right)\left(\dfrac{1}{r_\mathrm{e}^2} - \dfrac{1}{r_\mathrm{f}^2}\right)} \\
C_1 &= C_2\frac{1-2\nu}{r_\mathrm{i}^2} \\
C_1^{'} &= \frac{1-2\nu}{r_\mathrm{e}^2}\left[\left(\frac{1+\nu}{1-\nu}\alpha\frac{1}{r_\mathrm{f}}M_2 - M_1 r_\mathrm{f}\right)\frac{1}{M_3} + C_2\left((1-2\nu)\frac{r_\mathrm{f}}{r_\mathrm{i}^2} + \frac{1}{r_\mathrm{f}}\right)\frac{1}{M_3}\right] + M_1 \\
C_2^{'} &= \left(\frac{1+\nu}{1-\nu}\alpha\frac{1}{r_\mathrm{f}}M_2 - M_1 r_\mathrm{f}\right)\frac{1}{M_3} + C_2\left((1-2\nu)\frac{r_\mathrm{f}}{r_\mathrm{i}^2} + \frac{1}{r_\mathrm{f}}\right)\frac{1}{M_3}
\end{aligned} \tag{5}$$

where:

$$M_1 = \frac{(1+\nu)(1-2\nu)}{1-\nu}\frac{\alpha}{r_e^2}\frac{T_f}{2}\left(r_e^2 - r_f^2\right)$$

$$M_2 = \frac{T_i - T_f}{\ln\frac{r_i}{r_f}}\left(\frac{r_f^2}{2}\ln(r_f) - \frac{r_f^2}{4} - \frac{r_i^2}{2}\ln(r_i) + \frac{r_i^2}{4} - \frac{\ln(r_f)}{2}r_f^2 + \frac{\ln(r_f)}{2}r_i^2\right) + \frac{T_f}{2}\left(r_f^2 - r_i^2\right) \quad (6)$$

$$M_3 = (1-2\nu)\frac{r_f}{r_e^2} + \frac{1}{r_f}$$

Figure 12 shows the stress in radial, hoop and axial direction. A cylinder free to expand in axial direction is considered (this condition is the most similar to the actual mould state) and therefore a uniform axial stress needs to be superposed in the third of Eq. (3) in order to obtain a null resultant force at the ends.

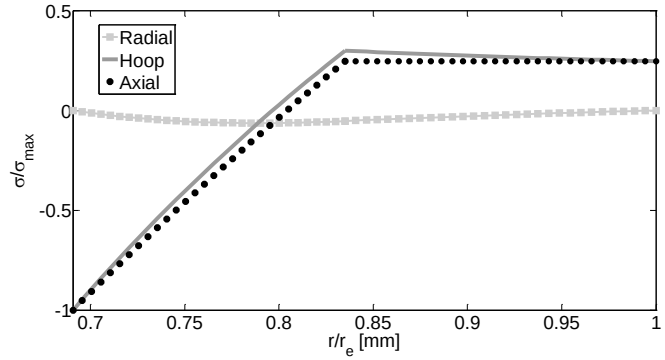

Figure 12. Stress distribution according to the proposed structural model.

By comparing Figure 12 with Figure 9 it is possible to notice a significant similarity especially in the more stressed area. Similar results have been obtained imposing the actual thermal flux to a hollow cylinder and comparing the stress distribution along a path parallel to the component axis and passing through point A.

In conclusion, from a thermal stress point of view, temperature produces a stress distribution characterized by two critical zones, respectively, close to the fillet and in the hottest region. In the first case this is due to the thermal moment produced by the temperature gradient which acts on a curved beam-like structure. In the second and most critical case the high compressive stresses occurring in the inner surface are due to the constraining effect imposed by the outer cold part. This behaviour can be well described by a simple analytical model, which refers to a hollow cylinder.

6. THERMO-MECHANICAL ANALYSIS UNDER CYCLING LOADS AND LIFE ASSESMENT

Figure 13 shows the stress-strain relation in point A when the mould undergoes the two types of load cycles; only "hoop" stresses are reported, since similar trends can be obtained considering axial stresses. In the case of the "start-up and switch-off" cycles, after the first heating, a compressive stress is produced which strongly exceeds the yield strength of the material. In the subsequent cooling phase (point 3 of Figure 4) residual tensile stresses are produced. A value of equivalent stress slightly higher than the yield stress of the material is reached. The subsequent cycles are therefore characterized by the typical elastoplastic hysteretic loop. In the case of the micro cycles due to the meniscus oscillation, a similar behaviour is produced, but in this case the yield stress of the material is exceeded only in the first heating, therefore the following cycles occur only in the elastic domain.

The durability of the critical zone in the inner part of the mould was then considered. As the component undergoes cyclic strains and stresses induced by thermal loads and plastic deformations occur, a strain-based thermal fatigue approach can be adopted. The durability analysis of continuous casting moulds is deeply investigated in literature [6, 10, 11, 12]. As it is well known [4] the usual method to relate strain and life refers to the evaluation of the plastic strain range which the material undergoes. In this work a different approach has to be followed. In fact, as previously pointed out, the plastic component of strain is significant only in the case of the macro-cycles. Moreover a more general remark has to be introduced. In fact the mechanical component here considered is characterized by self-imposed constrained thermal expansion as a consequence of cyclic temperature gradients. It follows that the total strain depends only on temperature distribution and it is independent from the elastoplastic model of the material. On the contrary, the relative amount of plastic and elastic strain is strongly influenced by the material model implemented to perform the numerical analysis. Therefore simplified elastoplastic models usually adopted (kinematic or isotropic hardening, etc.) could lead to different results in term of plastic strain. Recently, more accurate models (i.e. mixed kinematic isotropic) have been proposed in literature [13]. When strains are due to the combination of mechanical and thermally induced loads, these methods are probably the only choice to obtain accurate results in terms of plastic strain range. On the other hand, in the particular case described in this work, such approach seems to be of less practical support. This is due to the fact that, as the stabilized stress-strain cycle has to be obtained, a unfeasible computational effort would be required. In addition, in the present study cyclic (stabilized) material properties were not experimentally assessed.

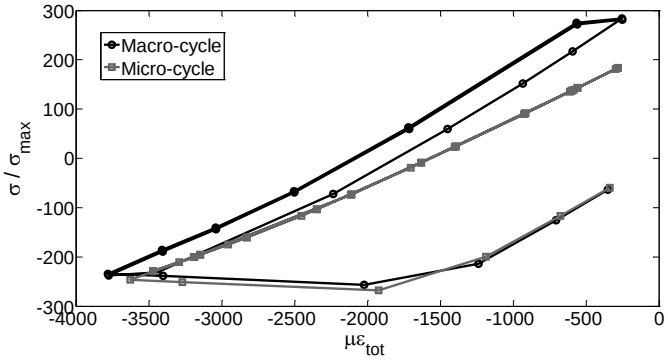

Figure 13. Stress-strain macro-cycles and micro-cycles

According to the previous consideration a total strain range approach, as suggested in [14, 15] is adopted. It is therefore necessary to introduce a suitable relation between total strain range and number of cycles to failure. Such relation is proposed in [14] and it consists of two power-law terms, one for the plastic strain, and the other for the elastic strain:

$$\Delta\varepsilon_{\text{tot}} = \Delta\varepsilon_{\text{el}} + \Delta\varepsilon_{\text{pl}} = XN_{\text{f}}^{\text{x}} + YN_{\text{f}}^{\text{y}} \tag{7}$$

where $\Delta\varepsilon_{\text{tot}}$ is the total strain range; X, x and Y, y are the coefficient and exponent terms relating to elastic ($\Delta\varepsilon_{\text{el}}$) and plastic ($\Delta\varepsilon_{\text{pl}}$) strain range respectively; N_{f} represents the number of cycles to failure.

All the coefficients and exponents proposed in Eq.(7) need to be determined experimentally; in the case of the copper alloy considered in this work experimental data of low cycle-fatigue test are available in terms of plastic strain only [6]. Other works present correlation between total strain range and life, but in different temperature-testing conditions or for different copper alloys [12, 10].

The Universal Slopes method proposed in [16] could be a alternative approach of practical use. In fact it relates only parameter obtained from tensile test (ultimate tensile strength, ductility, and modulus of elasticity) to fatigue life for a given strain range. According to this approach, for all materials the elastic and plastic lines have slopes of 0.12 and 0.6, respectively. One point on each of these two lines is determined considering the intersection on the strain axis at N_{f} equal to 1.0. For the elastic line, this intersection point depends only on the parameter S_{UTS}/E where S_{UTS} is the ultimate tensile strength, and E is the elastic modulus. For the plastic line, the intersection point is related only on ductility, defined as:

$$D = \ln\left(\frac{100}{100 - \%RA}\right) \tag{8}$$

where *RA* is the area reduction in a tensile test. According to Universal Slopes method, Eq.(1) becomes:

$$\Delta\varepsilon_{\text{tot}} = \left(3.5\frac{S_{\text{UTS}}}{E}\right)N_{\text{f}}^{-0.12} + D^{0.6}N_{\text{f}}^{-0.60} \tag{9}$$

As previously stated, a life estimation of the inner part of the mould has to be performed. In this region a biaxial stress state occurs, thus an equivalent strain range has to be computed, according to:

$$\Delta\varepsilon_{\text{eq}} = \frac{\sqrt{2}}{3}\sqrt{\left[\Delta(\varepsilon_1 - \varepsilon_2)\right]^2 + \left[\Delta(\varepsilon_1 - \varepsilon_3)\right]^2 + \left[\Delta(\varepsilon_2 - \varepsilon_3)\right]^2} \tag{10}$$

where $\Delta(\varepsilon_{\text{i}} - \varepsilon_{\text{j}})$ is the range of the relative difference between principal strains ε_{i} and ε_{j}. The elastic part in Eq.(9) must be consequently corrected as suggested in [14], while the plastic line remains unchanged. The curve for total strain range is thus displaced slightly downward, the displacement being the greatest in the region of high-cycle fatigue where the elastic component dominates. The following relation is finally obtained:

$$\Delta\varepsilon_{\text{eq}} = \frac{2}{3}(1+\nu)\left(3.5\frac{S_{\text{UTS}}}{E}\right)N_{\text{f}}^{-0.12} + D^{0.6}N_{\text{f}}^{-0.60} \tag{11}$$

At elevated temperatures, where creep and environmental interaction may occur, this method has been found to be non-conservative. As it is suggested in [16] this is due to the fact that intercrystalline cracking essentially bypasses the large number of cycles required to initiate a crack in the sub-creep range. Experimental tests on a wide range of materials point out that approximate results could be obtained by assuming that life under creep and environmental interaction conditions could cause as much as 90% loss of cyclic life, leaving only 10% of that calculated by the Universal Slopes Method, thus giving rise to the development of the so called 10% rule. The Universal Slopes Equation gives the upper-bound life, while the 10% rule gives the lowest expected life. Median expected life is estimated to be two times the lower bound life. The advantage of this method is its simplicity, since only the tensile properties need to be known at the desired temperature. Although accuracy is limited, the uncertainty related to measurements justifies this approach.

The resulting curve is plotted in Figure 14. Values proposed in literature for copper alloy with chemical composition that only slightly differs from

that of the material used in this work are also reported. It can be noticed that the curve proposed in [10] refers to a series of test performed at room temperature; these data fits well with the Universal Slopes Equation without temperature correction. In [12] experimental test were performed at 300°C; also in this case the obtained results are in good agreement with USE corrected with the 10% rule. These comparison seems therefore to confirm the correctness of the procedure proposed in this work.

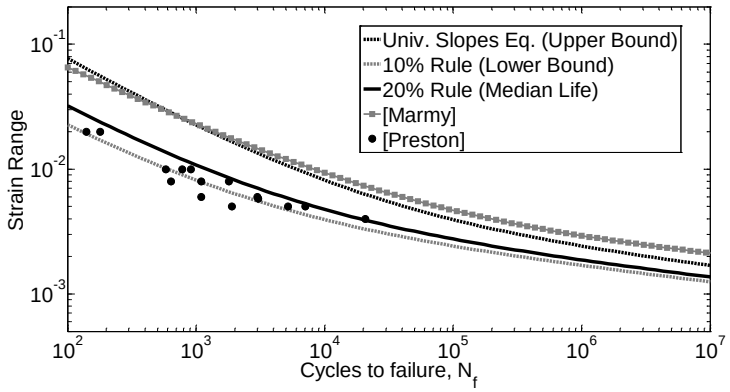

Figure 14. Equivalent strain range versus cycles to failure.

The results of the durability analysis are summarized in Table 2. It can be noticed that the number of cycles to failure is strongly lower in the case of the macro-cycle, characterized by a higher level of total strain range. On the other hand this result could be misleading. In fact, in a single operating sequence characterized by a start up and a switch off, a huge amount of micro-cycles occurs, due to the high frequency of the meniscus oscillation. Therefore, a lower number of sequences is obtained from micro-cycles.

Table 2: results of the durability analysis

	frequency	$\Delta\varepsilon_{eq}$	N° cycles	N° sequences
Macro cycle	1/20 hours	0.0040	6358	6358
Micro cycle	0.25 Hz	0.0027	25350	1.5

In conclusion, the durability of the component has to be evaluated in term of casting sequences; from this point of view it can be noticed that an opposite result is obtained, i.e. in the failure analysis of the component, strain range produced by the micro-cycle loads has to be primarily accounted for.

7. CONCLUSIONS

This work deals with the thermo-mechanical analysis of a copper mould. The mechanical behaviour of the component under thermal loading condition is analyzed adopting a three-dimensional finite-element model, with the aim of performing an accurate evaluation of stresses and strains levels. Two critical zones have been detected, respectively in the hottest region of the inner surface (point A) and close to the corner (point B). An analytical structural model is then developed with the aim of performing a sensitivity analysis in the design phase. A curved beam model seems suitable to describe the stress distribution around the corner (point B). A hollow cylinder with an imposed temperature distribution fits the hydrostatic plane stress status observed at the mid-face surface close to the meniscus region (point A). Using static tensile tests data performed on specimens obtained from actual mould, durability curves have been obtained adopting the Universal Slopes Method. The values of the total strain ranges for the two stress-strain cycles that characterize the component operation have been finally evaluated, estimating the lifespan of the component either in terms of number of cycles and in terms of casting sequences.

The developed models could be a useful support for the prediction of the residual life in real operation if the tracking of the component load history is performed; moreover the effective evaluation of different design improvement strategies can be also achieved.

REFERENCES

1. J. K. Park, B.G. Thomas, I.V. Samarasekera. Analysis of thermomechanical behaviour in billet casting with different mould corner radii, *Ironmaking and Steelmaking*, 29:1–17, 2002.
2. A. Weronski, and T. Hejwowski. Thermal Fatigue of Metals, Marcel Dekker, New York, 1991.
3. J. K. Park, B. G. Thomas, I. V. Samarasekera, U. S. Yoon. Thermal and mechanical behavior of copper molds during thin-slab casting (I): plant trial and mathematical modeling. *Metallurgical and Materials transactions*, 33B: 1–12, 2002.
4. J. K. Park, B. G. Thomas, I. V. Samarasekera, U. S. Yoon. Thermal and mechanical behavior of copper molds during thin-slab casting (II): mold crack formation. *Metallurgical and Materials transactions*, 33B: 437–449, 2002.
5. I. V. Samarasekera, D. L. Anderson, J.K. Brimacombe. The thermal distortion of continuous-casting billet molds. *Metallurgical Transactions* 13B: 91–104, 1982.

6. T. G. O'Connor and J. A. Dantzig. Modeling the thin-slab continuous-casting mold. *Metallurgical and Materials Transactions*, 25B: 443–457, 1994.
7. ITER Material Properties Handbook, ITER Doc. No. G 74 MA 9 01-07-11 W 0.2, Publication Package No. 7, 2001.
8. E. Winkler. Formänderung und Festigkeit gekrümmter Körper, insbesondere der Ringe. *Der Civilingenieur*, 4, 232–246, 1858.
9. S. Timoshenko and J. N. Goodier. Theory of elasticity. McGraw-Hill, 1952.
10. P. Marmy and O. Gillia. Investigations of the effect of creep fatigue interaction in a Cu-Cr-Zr alloy. *Proc. Engineering* 2: 407–416, 2010.
11. A. A. F. Tavassoli. Materials design data for fusion reactors. *J Nuclear Materials*, 258–263, 85–96, 1998.
12. S. D. Preston, I. Bretherton , C. B. A. Forty. The thermophysical and mechanical properties of the copper heat sink material intended for use in ITER. *Fusion Engineering and Design* 66 – 68, 441– 446, 2003.
13. J. H. You, M. Miskiewicz. Material parameters of copper and CuCrZr alloy for cyclic plasticity at elevated temperatures. *Journal of Nuclear Materials* 373, 269–274, 2008.
14. S. S. Manson. Thermal stress and low-cycle fatigue, McGraw-Hill, 1966.
15. J. A. Graham. Fatigue Design Handbook, *Advances in Engineering*, Vol. 4, Soc. of Automotive Engineers (SAE), 1968.
16. S. S. Manson, G. R. Halford. Fatigue and durability of structural materials, ASM International, 2006.